Conserved Ca^{2+}-antagonist-binding properties and putative folding structure of a recombinant high-affinity dihydropyridine-binding domain

Irene HUBER*, Edwin WAPPL*, Alexander HERZOG†, Jörg MITTERDORFER*, Hartmut GLOSSMANN*, Thierry LANGER† and Jörg STRIESSNIG*[1]

*Institut für Biochemische Pharmakologie, Peter-Mayrstrasse 1, A-6020 Innsbruck, Austria, and †Institut für Pharmazeutische Chemie, Innrain 52a, A-6020 Innsbruck, Austria

Sensitivity to 1,4-dihydropyridines (DHPs) can be transferred from L-type (α1C) to non-L-type (α1A) Ca^{2+} channel α1 subunits by the mutation of nine pore-associated non-conserved amino acid residues, yielding mutant $\alpha1A_{DHP}$. To determine whether the hallmarks of reversible DHP binding to L-type Ca^{2+} channels (nanomolar dissociation constants, stereoselectivity and modulation by other chemical classes of Ca^{2+} antagonist drugs) were maintained in $\alpha1A_{DHP}$, we analysed the pharmacological properties of (+)-[^{3}H]isradipine-labelled $\alpha1A_{DHP}$ Ca^{2+} channels after heterologous expression. Binding of (+)-isradipine (K_i 7.4 nM) and the non-benzoxadiazole DHPs nifedipine (K_i 86 nM), (±)-nitrendipine (K_i 33 nM) and (±)-nimodipine (K_i 67 nM) to $\alpha1A_{DHP}$ occurred at low nanomolar K_i values. DHP binding was highly stereoselective [25-fold higher affinity for (+)-isradipine]. As with native channels it was stimulated by (+)-*cis*-diltiazem, (+)-tetrandrine and mibefradil. This suggested that the three-dimensional architecture of the channel pore was maintained within the non-L-type α1A subunit. To predict the three-dimensional arrangement of the DHP-binding residues we exploited the X-ray structure of a recently crystallized bacterial K^+ channel (KcsA) as a template. Our model is based on the assumption that the Ca^{2+} channel S5 and S6 segments closely resemble the KcsA transmembrane folding architecture. In the absence of three-dimensional structural data for the α1 subunit this is currently the most reasonable approach for modelling this drug-interaction domain. Our model predicts that the previously identified DHP-binding residues form a binding pocket large enough to co-ordinate a single DHP molecule. It also implies that the four homologous Ca^{2+} channel repeats are arranged in a clockwise manner.

Key words: Ca^{2+} channel blocker, drug receptor, mutagenesis.

INTRODUCTION

Voltage-gated Ca^{2+} channels (VGCCs) mediate the depolarization-induced entry of Ca^{2+} into electrically excitable cells and thereby control essential physiological processes. Two different classes of high-voltage-activated Ca^{2+} channels can be distinguished pharmacologically: L-type Ca^{2+} channels (LTCCs), which are highly sensitive to different chemical classes of organic Ca^{2+} channel blockers ['Ca^{2+} antagonists', such as 1,4-dihydropyridines (DHPs), phenylalkylamines (PAAs) and benzothiazepines (BTZs)], and non-L-type channels (P-type, Q-type, N-type and R-type). The latter do not display Ca^{2+} antagonist sensitivity but are selectively inhibited by different peptide toxins [1]. DHPs, PAAs and BTZs are used clinically to treat cardiovascular diseases. In contrast, selective non-peptide blockers for non-L-type channels have not yet been described, although they might represent interesting drugs to treat severe pain, cerebral ischaemia (N-type channel blockers) [2] or migraine (P-type/Q-type channel modulators) [3].

L-type and non-L-type Ca^{2+} channels exist as hetero-oligomeric complexes of at least one α1, β and α2-δ subunit [4,5]. Different highly homologous α1 subunits form the Ca^{2+}-selective pore of the various Ca^{2+} channel types, resulting in different pharmacological properties. LTCCs contain α1C, α1D or α1S subunits that mediate a high affinity for Ca^{2+} antagonists. In contrast, P-type/Q-type and N-type Ca^{2+} channels contain α1A and α1B subunits respectively, which are insensitive to DHPs.

The development of selective non-L-type Ca^{2+} channel modulators might be considerably facilitated by understanding how DHPs, PAAs and BTZs interact with LTCC α1 subunits at the molecular level. Therefore residues critical for the formation of the high-affinity DHP-, PAA- and BTZ-binding domains on L-type α1 subunits (α1C, α1D or α1S) were identified with the use of site-directed mutagenesis (reviewed in [6,7]). A 'multisubsite-domain' model was proposed that predicted that these chemically unrelated drugs bind in close proximity to each other and next to the pore as well as to the channel's selectivity filter [7].

So far, molecular models of these drug-interaction domains could not be developed owing to the absence of three-dimensional structural information for Ca^{2+} channel α1 subunits. Such models would provide a useful basis for the further molecular analysis of the channel–drug interaction and could support the development of selective non-L-type channel blockers. The X-ray three-dimensional structure of a bacterial K^+ channel (KcsA) has recently been solved [8]. Its pore-forming transmembrane helices share sequence homology with the family of voltage-gated K^+, Na^+ and Ca^{2+} channels. KcsA is therefore believed to represent the prototype of the pore of these channels.

Here we provide evidence that the overall folding structure of different pore-forming channel subunits is likely to be very similar, by demonstrating that most of the DHP binding properties are preserved after transfer into DHP-insensitive α1A subunits (yielding a mutant subunit termed $\alpha1A_{DHP}$) [9,10]. By assuming that the three-dimensional architecture of the transmembrane pore helices of LTCC α1 subunits resembles the KcsA pore, we used the KcsA X-ray structure as a unique template to predict the three-dimensional arrangement of the DHP-binding residues. This effort was encouraged by previous work on seven-

Abbreviations used: BTZ, benzothiazepine; DHPs, 1,4-dihydropyridines; LTCCs, L-type Ca^{2+} channels; PAA, phenylalkylamine; VGCCs, voltage-gated Ca^{2+} channels.

[1] To whom correspondence should be addressed (e-mail joerg.striessnig@uibk.ac.at).

helix receptors for which useful drug receptor models were developed on the basis of the three-dimensional structure of bacteriorhodopsin [11].

The resulting model predicts a binding pocket that can accommodate a single DHP molecule with high affinity. In addition, our model suggests that the homologous repeats of VGCCs are arranged in a clockwise orientation.

EXPERIMENTAL

Materials

(+)-[^{3}H]Isradipine (PN 200-110) (approx. 80 Ci/mmol) was from New England Nuclear (Vienna, Austria), unlabelled isradipine enantiomers and racemic isradipine were from Sandoz (Basel, Switzerland), unlabelled verapamil enantiomers were from Knoll (Ludwigshafen, Germany), (+)-tetrandrine was a gift from Merck, Sharp and Dohme (Rahway, NJ, U.S.A.), (+)-*cis*-diltiazem was from Gödecke (Freiburg, Germany), and unlabelled mibefradil was a gift from Hoffmann–La Roche (Basel, Switzerland). Stock solutions of all unlabelled drugs were prepared in DMSO.

Heterologous expression in tsA201 cells

Human tsA201 cells (a human-embryonic-kidney-cell-derived cell line stably transfected with simian virus 40 large T-antigen) were plated and grown in Dulbecco's modified Eagle's medium/Coon's F-12 medium (Gibco/BRL; Life Technologies) containing 10 % (v/v) fetal bovine serum and 2 mM L-glutamine. α1A [9], $\alpha1A_{DHP}$ [9] and α1C [12] subunits were expressed in tsA201 cells together with α2-δ and β1a [9] subunits. In co-transfection experiments, expression plasmids were combined at concentrations equimolar with a total DNA amount of 15 μg per 10 cm-diameter culture dish (10.5 μg of Ca^{2+} channel subunit DNA plus 4.5 μg of pUC18 carrier DNA). All cDNA species were in the expression plasmid pcDNA3 (Invitrogen). Cells at approx. 60–70 % confluence were transfected by precipitation with calcium phosphate. Cells were incubated at 37 °C for 2–3 days before being harvested.

Electrophysiological measurements

Oocyte injection and measurements of barium inward currents through Ca^{2+}-channel mutants with the two-electrode voltage-clamp technique were measured as described [9]. Inhibition by (±)-isradipine was measured at a holding potential of −80 mV.

Construction of mutant T1039A

Mutant T1393A (mutation of Thr-1039 to alanine) was introduced by PCR into a *Sfi*I–*Cla*I cassette of a *Xho*I–*Cla*I fragment (nt 1689–4925) of $\alpha1A_{DHP}$ subcloned into pBluescript SK$^+$. The mutation was reintroduced through a *Nhe*I–*Cla*I fragment (nt 3543 and 4925) into $\alpha1A_{DHP}$ in $pNKS_2$.

Membrane preparations

Preparation of rabbit skeletal muscle membranes was performed as described [13]. Membranes from transfected cells were prepared after homogenization in 10 mM Tris/HCl (pH 7.4)/0.2 mM PMSF/0.5 mM benzamidine/1 μM pepstatin A/2 mM iodacetamide/1 μg/ml leupeptin/1 μg/ml aprotinin/0.1 mg/ml trypsin inhibitor [12]. Expression of recombinant subunits was monitored in immunoblots by employing subunit-selective polyclonal sequence-directed antibodies [14].

Radioligand-binding

Binding experiments with the benzoxadiazole DHP (+)-[^{3}H]-isradipine were performed in binding buffer [50 mM Tris/HCl (pH 7.4)/0.1 mM PMSF; final assay volume 0.5 ml] with the membrane protein and radioligand concentrations indicated in the Figure legends. After incubation for 60 min at 22 °C, bound ligand was quantified by rapid filtration over GF/C Whatman glass-fibre filters [pretreated with 0.25 % (v/v) polyethylenimine] [14]. Inhibition and stimulation studies were performed in the absence (control) and presence of unlabelled Ca^{2+} antagonists. Non-specific binding was determined in the presence of 1 μM unlabelled (±)-isradipine. Inhibition data for nifedipine, (±)-nitrendipine and (±)-nimodipine were measured in the presence of a stimulatory concentration (3 μM) of mibefradil. Serial dilutions of unlabelled drugs were made in DMSO. Final DMSO concentrations in the incubation mixture did not exceed 1 % (v/v), which did not affect (+)-[^{3}H]isradipine binding.

Data analysis

Binding inhibition and stimulation data were computer-fitted to the general dose–response equation [15] to obtain IC_{50} or EC_{50} values and slope factors. Data are given as means ± S.E.M. for the indicated number of experiments. In experiments with $\alpha1A_{DHP}$ the radioligand concentration was below the estimated K_d. K_i values therefore closely correspond to the IC_{50} values. K_i values for the binding of (+)-[^{3}H]isradipine to skeletal muscle and α1C were calculated by using the Cheng and Prusoff equation [16] with the K_d for (+)-[^{3}H]isradipine determined in direct saturation studies.

Sequence alignment and molecular modelling

The sequence alignment is described in Figure 3. The X-ray structure coordinates of the KcsA K^+ channel were downloaded from the Brookhaven Protein Database (accession number 1BL8) and the following LTCC amino acid residues (numbering according to α1C-II) [17] were introduced into the corresponding positions of the KcsA sequence (the asterisk indicates residues conserved between α1A and α1C, which were therefore not mutated in $\alpha1A_{DHP}$): in IIIS5, Thr-1039, Gln-1043; in IIIS6, Tyr-1152*, Ile-1153, Ile-1156, Phe-1158*, Phe-1159*, Met-1161; in IVS6, Tyr-1463*, Met-1464, Ile-1471, Asn-1472*. Ile-1470 was not 'mutated' into KcsA as it is not required for high DHP sensitivity [18].

The molecular models were constructed and visualized with both the SYBYL 6.3 (Tripos Associates) and the INSIGHT95 (MSI) software running on Silicon Graphics workstations. For energy calculations an L-type sequence was introduced into all S5 and S6 segments. Calculations were performed on the basis of the molecular mechanics procedures (cvff force field) by using the fixed docking script within INSIGHT95. To calculate low-energy conformations of the bound DHP molecule, the complex between 'mutated' KcsA channel and ligand was subjected first to 100 steps of minimization followed by sequential randomized translation and rotation movement of the DHP molecule. This procedure was repeated more than 250000 times, leading to 11 highly similar conformers.

RESULTS

The transfer of nine non-conserved LTCC amino acid residues (listed in the Experimental section) into P/Q-type α1A subunits renders inward currents through the resultant mutant (termed $\alpha1A_{DHP}$) highly sensitive to stimulation or blocking by DHPs [9,10]. Although saturable high-affinity binding of (+)-[^{3}H]-

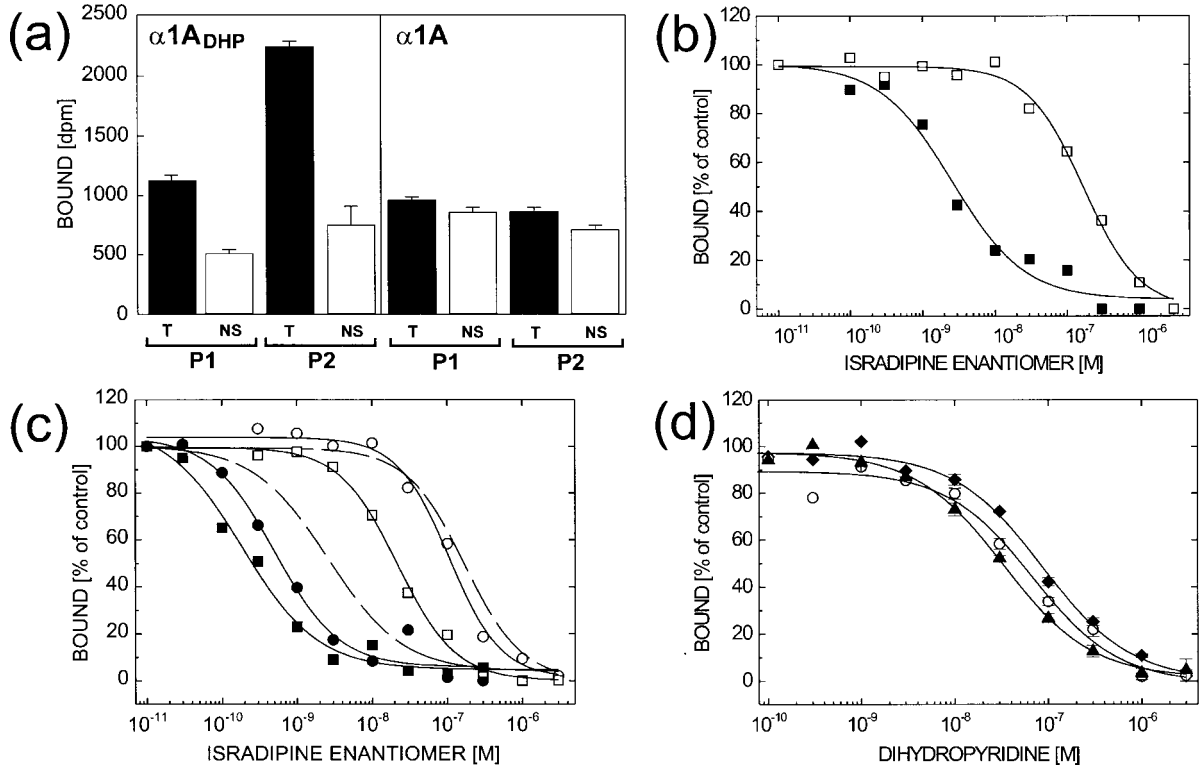

Figure 1 Binding of (+)-[^{3}H]isradipine to α1A$_{DHP}$

(**a**) Expression of saturable (+)-[^{3}H]isradipine binding in α1A$_{DHP}$: 0.7–1.0 nM (+)-[^{3}H]isradipine was incubated (60 min at 22 °C) with membrane protein from different preparations (P1, P2) of tsA201 cells transfected with α1A$_{DHP}$ or α1A together with α2-δ and β1 subunits. Total (T, black bars) and non-specific binding [NS, white bars, detected in the presence of 1 μM (±)-isradipine] were determined as described in the Experimental section. Membrane protein concentrations were 0.4 (P1) and 0.3 mg/ml (P2). Means ± range for duplicate determinations are given. Two of four similar experiments are shown for each α1 construct. (**b**) Stereoselective inhibition of (+)-[^{3}H]isradipine binding to α1A$_{DHP}$ by (+)-isradipine and (−)-isradipine: the ligand concentration was 0.74 nM; membrane protein concentration was 0.3 mg/ml. One of six or seven similar experiments is shown. Binding parameters: (+)-isradipine (■), IC_{50} = 2.6 nM, slope = 0.87; (−)-isradipine (□), IC_{50} = 169 nM, slope = 1.12. (**c**) Stereoselective inhibition of (+)-[^{3}H]isradipine binding to α1S and α1C. Binding to rabbit skeletal muscle membrane protein (7 μg/ml) and heterologously expressed α1C membrane protein (130 μg/ml) was measured in the absence or presence of increasing concentrations of isradipine enantiomers. Radioligand concentrations were 0.15 nM (rabbit skeletal muscle) and 0.20 nM (α1C). For α1A$_{DHP}$ inhibition, data from (**b**) are shown for comparison (broken lines). Binding parameters for rabbit skeletal muscle membranes: (+)-isradipine (●), IC_{50} = 0.63 nM, slope = 1.05; (−)-isradipine (○), IC_{50} = 103 nM, slope = 1.20. Binding parameters for α1C: (+)-isradipine (■), IC_{50} = 0.18 nM, slope = 0.99; (−)-isradipine (□), IC_{50} = 21.5 nM, slope = 1.13. (**d**) Inhibition of (+)-[^{3}H]isradipine binding to α1A$_{DHP}$ by non-benzoxadiazole DHPs [nifedipine, (±)-nimodipine and (±)-nitrendipine]. Radioligand and membrane protein concentrations were 0.9–1.1 nM and 0.3–0.4 mg/ml respectively. Data from six almost identical independent experiments were pooled and then computer-fitted to the general dose–response curve. Nifedipine (◆), IC_{50} = 85.8 nM, slope = 0.91; (±)-nimodipine (○), IC_{50} = 67.3 nM, slope = 0.95; (±)-nitrendipine (▲), IC_{50} = 32.8 nM, slope = 0.92.

isradipine was also demonstrated for α1A$_{DHP}$ expressed in tSA201 cells [10], it is so far unclear whether this recombinant binding domain also maintains other characteristic pharmacological features in radioligand-binding experiments. In addition to stereoselectivity and high affinity for other DHPs we therefore investigated whether the typical non-competitive modulation of DHP binding by other chemical classes of Ca^{2+} antagonists was also transferred by the mutations.

Figure 1(a) illustrates that specific (+)-[^{3}H]isradipine binding appears after the expression of α1A$_{DHP}$, together with α2-δ and β1 in tsA201 cell membranes. Binding is absent after the expression of α1A/α2-δ/β1. This is not due to a lack of expression of α1A, because α1A and α1A$_{DHP}$ are expressed at similar protein levels, as revealed by immunoblot experiments with a sequence-directed antibody recognizing both subunits (results not shown). Additional immunocytochemical staining of transfected cells also showed no difference in channel targeting to the plasma membrane (results not shown).

At radioligand concentrations between 0.5 and 1.6 nM, binding increased linearly up to a membrane protein concentration of 0.5 mg/ml (results not shown). Specific binding was doubled when radioligand concentrations were increased from 0.8 to 1.6 nM, suggesting that the K_d must have been well above 0.8 nM. The affinity (given as K_i) for isradipine and other DHPs was therefore estimated from binding-inhibition experiments (Figure 1b).

Specific binding was inhibited by the unlabelled enantiomers of isradipine in a highly stereoselective manner, the (+)-enantiomer being 25-fold more potent than the (−)-enantiomer (Figure 1b, Table 1). The affinity of (+)-isradipine for the recombinant site on α1A$_{DHP}$ was 76-fold lower than for the DHP-binding domain of heterologously expressed α1C, but only 10-fold lower than for native skeletal muscle Ca^{2+} channels (Table 1, Figure 1c). In contrast, the affinity for the (−)-enantiomer was only 1.4–8.5-fold lower than in skeletal muscle and in α1C. The non-benzoxadiazole DHPs nifedipine, (±)-nitrendipine and (±)-nimodipine (Table 1, Figure 1d) also displayed nanomolar affinity for α1A$_{DHP}$. From the respective K_d values we calculated binding energies for (+)-isradipine of 51.9 kJ/mol (12.43 kcal/mol) for skeletal muscle channels (α1S) and 46.2 kJ/mol (11.05 kcal/mol) for α1A$_{DHP}$. These results demonstrate that the recombinant site supports high-affinity

Table 1 Modulation of (+)-[^{3}H]isradipine binding to $\alpha 1A_{DHP}$ by Ca^{2+} antagonists

IC_{50} values for inhibition and EC_{50} values for stimulation are given (as means ± S.E.M. for $n \geqslant 3$ or range for $n = 2$). Maximal inhibition or stimulation (given as a percentage of the control binding at infinitely high drug concentrations) are given in parentheses. Abbreviations: $\alpha 1C$, $\alpha 1C/\alpha 2\text{-}\delta/\beta$ expressed in tsA201 cell membranes; $\alpha 1S$, native skeletal muscle Ca^{2+} channels; n.d., not determined.

	IC_{50} or EC_{50} (nM)	
Modulator	$\alpha 1A_{DHP}$	L-type $\alpha 1$
(+)-Isradipine	7.4 ± 2.9 (0%)	0.10 ± 0.01 ($\alpha 1C$)*
		0.72 ± 0.24 ($\alpha 1S$)*
(−)-Isradipine	187 ± 48 (0%)	11 ± 1 ($\alpha 1C$)*
		130 ± 47 ($\alpha 1S$)*
Nifedipine	85.8* (0%)†	8.2 ($\alpha 1C$)‡
(±)-Nimodipine	67.3* (0%)†	6.7 ($\alpha 1S$)§
(±)-Nitrendipine	32.8* (0%)†	4.9 ($\alpha 1S$)‖
(+)-*cis*-Diltiazem	3100 ± 1300 (285 ± 12%)	910 ± 150 nM (135 ± 6%) ($\alpha 1C$)¶
(+)-Tetrandrine	n.d. (369 ± 48%)	n.d (281 ± 101%) ($\alpha 1C$)*
Mibefradil	324 ± 1 (333 ± 22)	156 ± 17 (141 ± 5) ($\alpha 1C$)*

* This paper.
† IC_{50} derived by computer fitting of pooled data from three independent experiments.
‡ Data taken from [37].
§ Data taken from [38].
‖ Data taken from [39].
¶ Pig heart membranes.

(+)-isradipine binding with only 10% less binding energy than for native skeletal muscle LTCCs.

Another unique feature of the DHP-binding domain of LTCCs is their non-competitive modulation by other chemical classes of Ca^{2+} antagonists, such as PAAs and BTZs. This would require not only that the high-affinity binding domains for these drugs are also present in $\alpha 1A_{DHP}$ but that the overall conformation of the channel pore is similar to LTCCs, allowing steric or allosteric drug interaction with the concomitantly bound DHP molecule.

As two of the nine amino acid residues (Tyr-1463 and Ile-1470) transfer crucial BTZ-binding determinants [19], we tested whether drugs interacting with this domain, (+)-*cis*-diltiazem and (+)-tetrandrine [20], are able to stimulate (+)-[^{3}H]isradipine binding, as in $\alpha 1C$. As shown in Figure 2(a) and Table 1, this is indeed so. We also tested the modulatory effect of the non-selective Ca^{2+} channel blocker mibefradil, which blocks L-type and non-L-type Ca^{2+} channels with similar affinities [21] and is therefore expected to bind to $\alpha 1A_{DHP}$ (and $\alpha 1A$) as well. Like (+)-*cis*-diltiazem, mibefradil stimulated (+)-[^{3}H]isradipine binding to both $\alpha 1C$ (Figure 2c) and $\alpha 1A_{DHP}$ (Figure 2a). Neither drug enhanced non-specific (+)-[^{3}H]isradipine binding to cells expressing $\alpha 1A$ ($n = 3$) or to mock-transfected cells ($n > 3$).

Since (+)-*cis*-diltiazem and mibefradil stimulated with comparable EC_{50} values in $\alpha 1A_{DHP}$ and $\alpha 1C$ (Figures 2a and 2c; Table 1) their binding domains seem to be well preserved in $\alpha 1A_{DHP}$.

Previous electrophysiological experiments have shown that Tyr-1463 and Ile-1470 also elicit partial PAA sensitivity in $\alpha 1A$ subunits [19]. We therefore tested whether the enantiomers of verapamil modulate DHP binding in $\alpha 1A_{DHP}$. (+)-[^{3}H]Isradipine binding to $\alpha 1A_{DHP}$ was stimulated by (−)- and (+)-verapamil (Figure 2b), whereas a characteristic partial inhibition [22] was observed for $\alpha 1C$ (Figure 2c). These experiments revealed that strong non-competitive coupling between the PAA- and DHP-binding domains was maintained in $\alpha 1A_{DHP}$ although a stimulatory rather than an inhibitory effect was observed in the recombinant binding domain.

Taken together, our experiments extend previous findings [9]

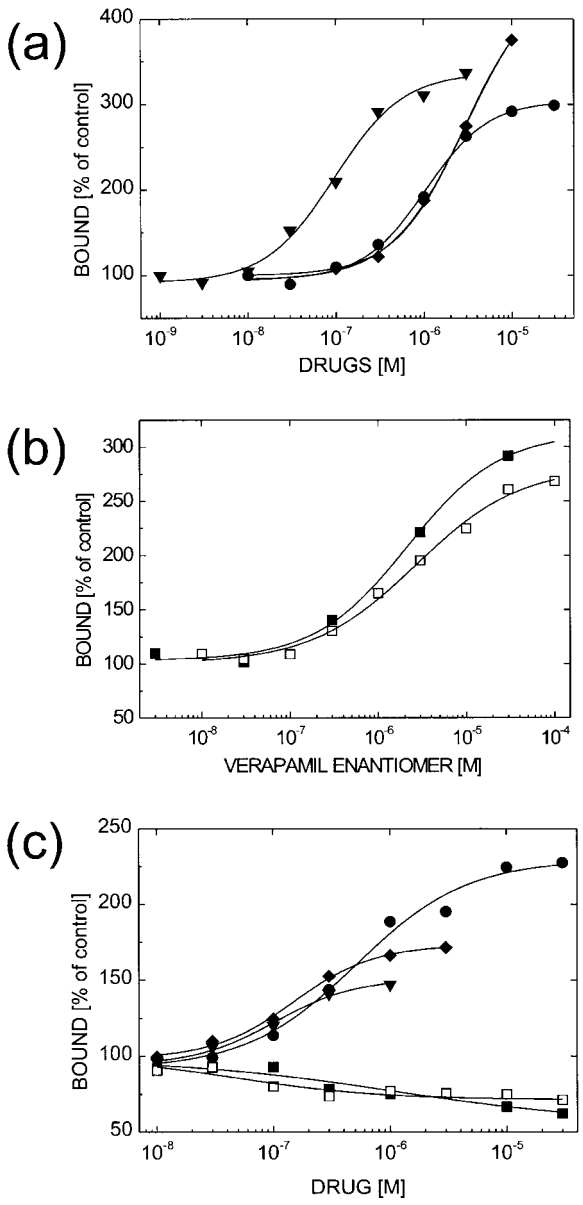

Figure 2 Modulation of (+)-[^{3}H]isradipine binding to $\alpha 1A_{DHP}$ (a,b) and $\alpha 1C$ (c) by mibefradil, (+)-*cis*-diltiazem, (+)-tetrandrine, and verapamil enantiomers

Radioligand and membrane protein concentrations were respectively 0.9–1.4 nM and 0.3 mg/ml for $\alpha 1A_{DHP}$, and 0.1–0.2 nM and 0.12–0.25 mg/ml for $\alpha 1C$. One of two or three similar experiments is shown. (**a**) (+)-*cis*-Diltiazem (●), $EC_{50} = 1.04\ \mu M$, stimulation to 304%; (+)-tetrandrine (◆), 3.03 μM, stimulation to 459%; mibefradil (▼), $EC_{50} = 96.4$ nM, stimulation to 337%. In the presence of a constant concentration of mibefradil (3 μM) the K_i of (+)-isradipine was decreased from 7.4 to 1.6–1.7 nM (range, $n = 2$). The binding stimulation by mibefradil can therefore be explained by an increase in binding affinity. (**b**) (+)-Verapamil (■), $EC_{50} = 2.2\ \mu M$, stimulation to 313%, (−)-verapamil (□), $EC_{50} = 2.7\ \mu M$, stimulation to 282%. (**c**) (+)-Verapamil (■), 1.06 μM, inhibition to 56%; (−)-verapamil (□), $IC_{50} = 49$ nM, inhibition to 72%; (+)-*cis*-diltiazem (●), $EC_{50} = 520$ nM, stimulation to 229%; (+)-tetrandrine (◆), $EC_{50} = 150$ nM, stimulation to 173%; mibefradil (▼), $EC_{50} = 103$ nM, stimulation to 151%.

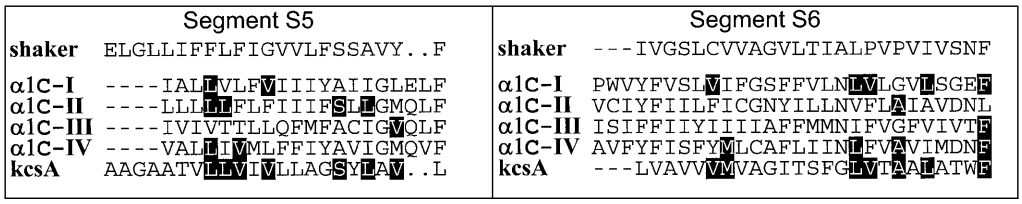

Figure 3 Sequence alignment of KcsA with the transmembrane S5 and S6 segments of voltage-gated Na^+, K^+ and Ca^{2+} channels

The sequence homology between LTCC α1C and KcsA is limited and complicates direct sequence alignment. We therefore first aligned the S5 and S6 segments of the four homologous rabbit α1C repeats with the corresponding segments of voltage-gated Na^+ channels (rat brain Na^+ channel II) [35]. Shaker K^+ channel sequence was then aligned to the Na^+-channel sequence as described [35]; finally, KcsA was aligned to the Shaker K^+ channel sequence as described [36]. Residues conserved between KcsA and one or more of the LTCC segments are highlighted.

by demonstrating that not only DHP sensitivity but also other hallmarks of DHP binding, such as stereoselectivity and non-competitive binding modulation by other chemically unrelated Ca^{2+} antagonists, are preserved in $\alpha 1A_{DHP}$. Thus the three-dimensional geometry of the DHP-binding residues after transfer into the α1A sequence environment must closely resemble their arrangement within the DHP-binding domain of L-type Ca^{2+} channel α1 subunits (e.g. α1C, α1S). It still allows the formation of the characteristic 'multisubsite' drug-binding pocket [7] to which different chemical classes of Ca^{2+} antagonists can bind at the same time and thereby affect each other's binding by steric and/or allosteric mechanisms.

The further structural refinement of these drug interactions will require the development of a molecular model of the DHP-binding pocket. Owing to their large size and the high hydrophobicity of α1 subunits, the three-dimensional structural information (from NMR studies and/or X-ray crystallography) is unlikely to be available in the near future.

However, the three-dimensional structure of a putative prototype of the pores of the voltage-gated cation channel family, the bacterial K^+ channel KcsA, has recently been resolved by X-ray crystallography [8]. KcsA contains only two membrane-spanning segments, which form homotetramers and, on the basis of sequence similarity and helix arrangement, closely resemble the pore-forming segments of voltage-gated cation channels [8,23]. On the basis of the above finding that the DHP-binding domain can be reconstituted within the structural framework of a related ion channel and by assuming that transmembrane KcsA helices predict the three-dimensional arrangement of the S5 and S6 segments of the VGCC α1 subunits reasonably well, we used the KcsA structure as a unique template to construct a model of the DHP-binding domain. In the absence of any other three-dimensional structural information about Ca^{2+} channel α1 subunits this is at present the most reasonable approach for deriving such a model.

Using molecular modelling we introduced the L-type DHP-binding residues into the KcsA sequence after their corresponding position had been determined by sequence alignment of KcsA with α1C as described in the Experimental section and Figure 3. The positions of the 12 DHP-binding residues (given in the Experimental section) within the KcsA sequence resulting from this alignment are shown in Figure 4. For clarity, KcsA amino acid side chains and hydrogen atoms are not displayed. Note that KcsA was crystallized as a homotetramer, whereas VGCCs consist of four homologous but not identical repeats tethered together by intracellular linkers. Therefore the α1 subunit sequence can be assigned to the KcsA tetramer by either a clockwise (Figure 4a) or counterclockwise (Figure 4b) arrangement. Note that at present no biochemical evidence is available that would permit any predictions to be made about whether the four membrane-spanning homologous repeats of voltage-gated Na^+ and Ca^{2+} channels are arranged in a clockwise or a counterclockwise direction. Therefore both possibilities had to be analysed in our model. Figure 4a (top view) illustrates that DHP-binding residues in IIIS5, IIIS6 and IVS6 can participate in the formation of a single binding pocket only after clockwise arrangement of repeats I–IV. In contrast, in a counterclockwise arrangement (Figure 4b, top view) IIIS5 and some of the IIIS6 residues form a very narrow cleft from which IVS6 residues are excluded. Therefore one interesting prediction from our model is that the homologous repeats of VGCCs are arranged in a clockwise manner. Figures 4(c)–4(e) show the position of the DHP-binding residues in the (preferred) clockwise model from different perspectives, together with the crystal structure of (+)-isradipine. If the flexibility of their side chains is taken into account, all amino acids can be oriented towards a common binding pocket with the exception of IIIS6 Phe-1159 (Figure 4a). This is in agreement with earlier studies demonstrating that this residue contributes only very weakly to DHP sensitivity [24]. The dimensions of the pocket (Figures 4c–4e) permit the accommodation of a single DHP molecule (see below). Its narrow inner portion is formed by residues Met-1161 (IIIS6) and Asn-1472 (IVS6), whose side chains are approx. 5.5 Å apart. This is close enough to form a hydrogen bond that could participate in the conformational stabilization of the pore region. The interaction of DHP with these residues could therefore permit the modulation of channel gating. The wider outer portion is formed by residues Tyr-1152 (IIIS6), Gln-1043 (IIIS5), Tyr-1463 and Met-1464 (IVS6). Gln-1043–Met-1464 and Gln-1043–Tyr-1463 are separated by approx. 10 Å. This is not close enough for hydrogen-bonding but both distances can easily be spanned by a DHP molecule (9 Å between the DHP ring nitrogen and the isopropyl side chain). Interestingly, most residues forming this outer portion (Gln-1043 [25]; Tyr-1463 and Met-1464 [26]) are essential for channel activation by DHP agonists (e.g. BayK 8644). It is therefore possible that pharmacophores that are important for agonist activity (e.g. for hydrogen-bonding) are oriented towards the outer portion of the pocket.

We also used our model to explain the marked decrease in affinity after the replacement of Thr-1039 by a tyrosine residue [26]. As shown in Figures 4(a) and 4(c), Thr-1039 points toward the centre of the binding pocket. Its distance from important drug-binding residues in IIIS6 (Met-1161) and IVS6 (Met-1464) is approx. 10 Å. The model would therefore predict that a more bulky tyrosine side chain, which is 3.9 Å longer than that of threonine, should interfere with the co-ordination of the DHP molecule in the centre of the binding pocket. If this were true, a less bulky residue should be tolerated in this position. To confirm

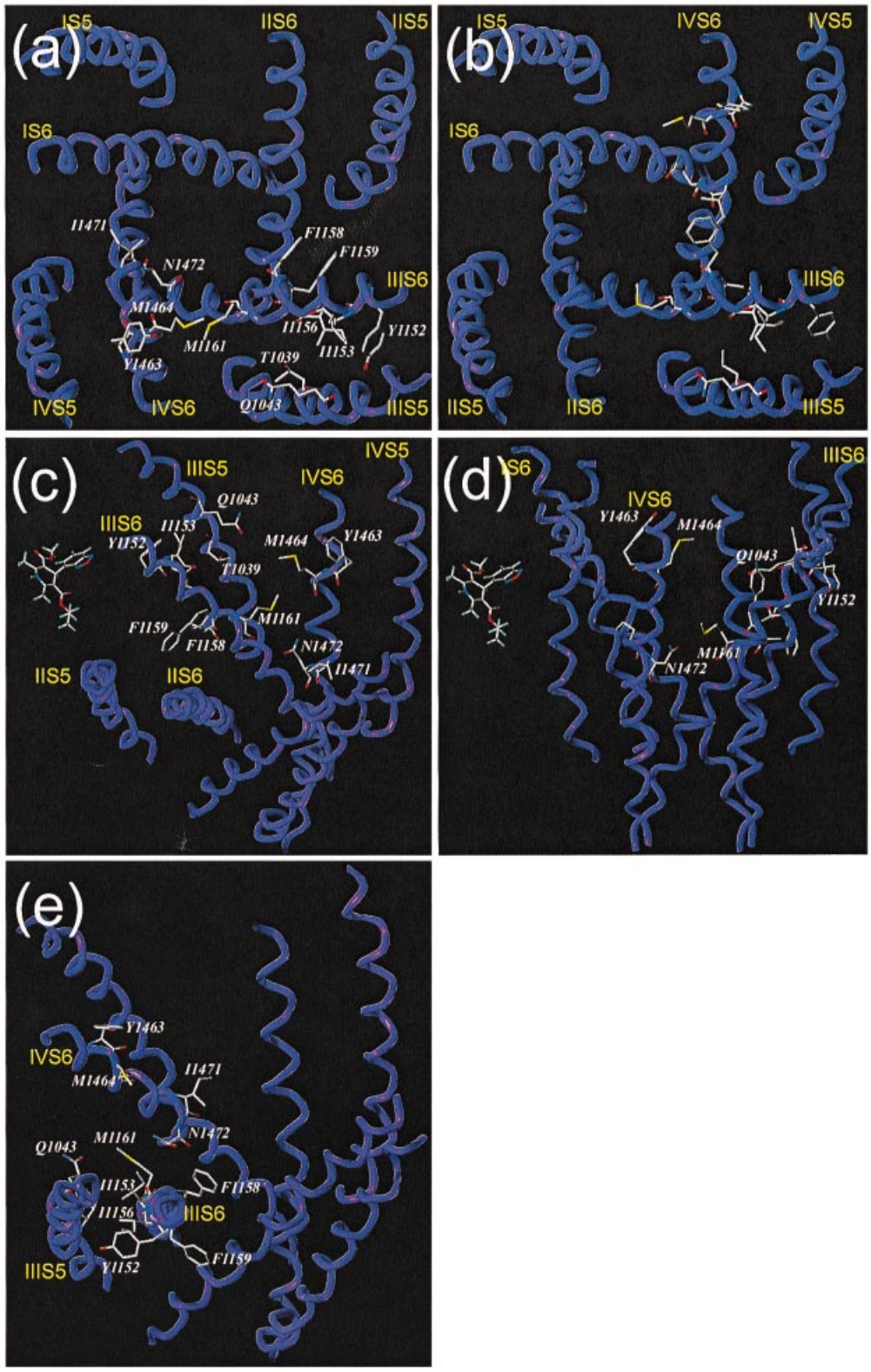

Figure 4 Molecular model of the DHP-binding domain

Residues previously identified as important for DHP sensitivity (see the text) were introduced into the KcsA sequence in accordance with the sequence alignment in Figure 3. Their side chains are displayed within the three-dimensional model based on the X-ray structure of KcsA after clockwise (**a**, **c**, **d**, **e**) and counterclockwise (**b**) assignment of the homologous Ca^{2+} channel repeats. For clarity, KcsA amino acid side chains and hydrogen atoms are not shown. Blue tubes connect backbone Cα atoms. (**a**, **b**). Top view along the axis of the pore; (**c**) view from the extracellular side along the axis of the IIS6 helix; (**d**) side view; (**e**) view from the extracellular side along the axis of the IIIS6 helix.

this prediction we replaced Thr-1039 in $\alpha 1A_{DHP}$ by alanine (T1039A), expressed the mutant channel in *Xenopus* oocytes and determined its sensitivity to isradipine. This mutation did not significantly affect sensitivity to isradipine [inhibition by 10 μM ($\pm$)-isradipine: $\alpha 1A_{DHP}$, $72 \pm 3\,\%$ of the control current ($n = 4$); T1039A, $60 \pm 5\,\%$ ($n = 5$; P 0.05] and therefore provides direct experimental evidence for the steric obstruction of the binding pocket by tyrosine. This finding is in excellent agreement with the prediction of our model.

We also investigated whether a DHP molecule could fit into the binding pocket generated in our 'mutated' KcsA channel in the presence of the pore-loop residues and with the complete L-type sequence introduced into the helices corresponding to IIIS5, IIIS6 and IVS6. To address this question we performed a preliminary docking calculation based on simple molecular mechanics procedures. Our preliminary experiments indicated that, in the presence of the pore loops, (1) the region spanned by the DHP-binding residues is able to accommodate one ligand molecule and (2) some of the amino acids known to interact with DHPs are located favourably for interactions with the ligand in energy-minimized conformations. This was true of Asn-1472, Ile-1471, Met-1464 and Phe-1158.

Our experiments provide a preliminary model of the DHP-binding domain that will be highly useful in analysing the structure–activity relationship of the interaction of DHP with its binding domain on the channel's α1 subunit in conjunction with mutational analysis.

DISCUSSION

Using radioligand binding we provide evidence that a recombinant DHP-binding domain mutated into a DHP-insensitive Ca^{2+}-channel subunit retains most fundamental properties typical of DHP interaction with LTCCs. We confirm the stereospecificity of isradipine interaction with $\alpha 1A_{DHP}$ observed functionally [9] at the biochemical level (i.e. unaffected by membrane voltage) and show that the non-benzoxadiazole DHPs ($\pm$)-nitrendipine, ($\pm$)-nimodipine and nifedipine can also interact with nanomolar K_d values. Although the affinity for DHPs is about an order of magnitude [approx. 10-fold for (+)-isradipine] lower than for skeletal muscle LTCCs, the estimated K_d values are still in the low nanomolar range. Interestingly, the decrease in affinity for the less potent (−)-isradipine was less pronounced. Recent studies with fluorescent Ca^{2+} antagonists indicate that DHP binding is a multistep process in which initial low-affinity complexes are formed by both enantiomers; further rearrangement to high-affinity complexes occurs only for the more active enantiomer [27,28]. It is possible that $\alpha 1A_{DHP}$ supports the formation of initial complexes for both isradipine enantiomers but allows a less complete rearrangement of the (+) enantiomer to form a high-affinity complex than for the skeletal muscle or cardiac channels.

In addition to the stereoselectivity and nanomolar affinity, the recombinant DHP pocket retained its ability to non-competitively interact with the binding domains of the chemically unrelated Ca^{2+} channel blockers (+)-*cis*-diltiazem, (+)-tetrandrine and verapamil. These drugs modulate DHP binding by steric and/or allosteric mechanisms [22,28], both of which result from drug interaction in very close proximity to the DHP-binding pocket. Although their domains are only partly restored by the mutations in $\alpha 1A_{DHP}$ their modulatory actions are very similar to those of LTCCs. The only difference that we observed was stimulation ($\alpha 1A_{DHP}$) rather than partial inhibition (α1C) by the verapamil enantiomers. However, this difference is apparent only because stimulatory effects of PAAs have also been reported for LTCC α1 subunits [29,30]. Taken together, our results indicate that the three-dimensional architecture within L-type and non-L-type α1 subunits must be very similar.

In the absence of precise three-dimensional structural information on α1 subunits, few approaches are available for predicting α1 subunit topology, including the molecular organization of the DHP-binding pocket. Therefore our approach to predicting the arrangement of the Ca^{2+} channel S5 and S6 segments on the basis of the crystal structure of KcsA is currently the most reasonable for deriving a working model for the further structural characterization of this drug-interaction domain. However, it is important to emphasize that the conclusions of our model are correct only if the assumption that the three-dimensional architecture of the α1 subunit S5 and S6 segments is predicted by KcsA is also correct.

In the KcsA-derived model the DHP-binding residues form a binding pocket that can accommodate a single DHP molecule. However, this is achieved only if the homologous repeats of the channel are arranged in a clockwise orientation. In the absence of other biochemical data this result emphasizes the suitability of small ligands as molecular rulers to provide a first insight into the molecular arrangement of these large proteins. Our results are in agreement with preliminary results obtained with a Na^+-channel toxin inferring a clockwise arrangement also in voltage-gated Na^+ channels [31].

It is known that the interaction of DHPs with LTCCs is highly voltage-dependent, owing to the higher affinity of DHPs for inactivated Ca^{2+} channels at depolarized membrane potentials (see, for example, [26]). For $\alpha 1A_{DHP}$ the voltage dependence of the interaction with DHP seems to be very limited because the IC_{50} for inhibition of mostly resting channels at −120 mV (13.8 nM [10]) is similar to the K_d measured in our binding experiments (7.4 nM). At present it is unclear how voltage-induced conformational changes translate into changes in DHP-binding affinity. They could result in movements of the S5 and S6 segments on channel gating, causing rearrangements of the DHP-binding residues. Alternatively, they could affect the access of DHPs to the binding domain [32].

Our model must be confirmed and refined by mutational analysis. Although the exact orientation of the DHP molecule in this pocket cannot be predicted, general properties of the binding domain can be tested. In the present study we showed that a tyrosine residue in position 1039 decreases DHP sensitivity by steric hindrance because even the small methyl side chain of an alanine in this position fully supported DHP sensitivity. This finding agrees with our model, which predicts that the bulky tyrosine side chain protrudes into the centre of the binding pocket and must therefore interfere with the co-ordination of the DHP molecule.

The availability of a refined model of the DHP-binding domain will not only provide valuable insight into the mechanism of channel blocking or activation by these drugs but also support the development of drugs with selectivity for non-L-type Ca^{2+} channels. Owing to the high homology of L- and non-L-type Ca^{2+} channel α1 subunits within this drug-binding region it is reasonable to speculate that structural modification of DHPs, PAAs and BTZs might result in drugs with selectivity for non-L-type Ca^{2+} channels. We consider DHPs to be the most promising candidates for several reasons: (1) DHPs penetrate the blood–brain barrier more easily than the cationic amphiphilic PAAs and BTZs; (2) some DHPs represent high-affinity Ca^{2+} channel activators, a property that might also be of pharmacological relevance for non-L-type Ca^{2+} channels; (3) unlike PAAs and BTZs, DHPs do not interact with other proteins unrelated to

Ca^{2+} channels (such as sigma-receptors and sterol isomerases) [33,34].

Our results pave the way for future mutational studies to refine our DHP binding model structurally.

We thank Dr Martina J. Sinnegger and Dr J. Platzer for helpful discussion, Dr G. Eaholtz for providing tsA201 cells, Dr B. E. Flucher and M. Hitzl for help with immunocytochemistry, Mr P. Eller for providing preliminary information on binding properties of mibefradil, and Ms D. Ostler and J. Meitz for expert technical assistance. This work was supported by grants from the Österreichische Nationalbank (to J.S.), the FWF (P12641 to J.S. and P12689 to H.G.) and the Dr Legerlotz Foundation.

REFERENCES

1 Birnbaumer, L., Campbell, K. P., Catterall, W. A., Harpold, M. M., Hofmann, F., Horne, W. A., Mori, Y., Schwartz, A., Snutch, T. P., Tanabe, T. and Tsien, R. W. (1994) The naming of voltage-gated calcium channels. Neuron **13**, 505–506

2 Miljanich, G. P. and Ramachandran, J. (1995) Antagonists of neuronal calcium channels: structure, function and therapeutic implications. Annu. Rev. Pharmacol. Toxicol. **35**, 707–734

3 Kraus, R. L., Sinnegger, M. J., Glossmann, H., Hering, S. and Striessnig, J. (1998) Familial hemiplegic migraine mutations change alpha1A calcium channel kinetics. J. Biol. Chem. **273**, 5586–5590

4 Catterall, W. A. (1995) Structure and function of voltage-gated ion channels. Annu. Rev. Biochem. **64**, 493–531

5 Gurnett, C. A. and Campbell, K. P. (1996) Transmembrane auxiliary subunits of voltage-dependent ion channels. J. Biol. Chem. **271**, 27975–27958

6 Hockerman, G. H., Peterson, B. Z., Johnson, B. D. and Catterall, W. A. (1997) Molecular determinants of drug binding and action on L-type calcium channels. Annu. Rev. Pharmacol. Toxicol. **37**, 361–396

7 Striessnig, J., Grabner, M., Mitterdorfer, J., Hering, S., Sinnegger, M. J. and Glossmann, H. (1998) Structural basis of drug binding to L calcium channels. Trends Pharmacol. Sci. **19**, 108–115

8 Doyle, D. A., Cabral, J. M., Pfuetzner, R. A., Kuo, A., Gulbis, J. M., Cohen, S. L., Chait, B. T. and MacKinnon, R. (1998) The structure of the potassium channel: molecular basis of K^+ conduction and selectivity. Science **280**, 69–77

9 Sinnegger, M. J., Wang, Z., Grabner, M., Hering, S., Striessnig, J., Glossmann, H. and Mitterdorfer, J. (1997) Nine L-type amino acid residues confer full 1,4-dihydropyridine sensitivity to the neuronal calcium channel alpha1A subunit: role of L-type methionine-1188. J. Biol. Chem. **272**, 27686–27693

10 Hockerman, G. H., Peterson, B. Z., Sharp, E., Tanada, T. N., Scheuer, T. and Catterall, W. A. (1997) Construction of a high-affinity receptor site for dihydropyridine agonists and antagonists by single amino acid substitutions in a non-L-type calcium channel. Proc. Natl. Acad. Sci. U.S.A. **94**, 14906–14911

11 Wieland, K., Zuumond, H. M., Krasel, C., Ijzerman, A. P. and Lohse, M. J. (1996) Involvement of Asn-293 in stereospecific agonist recognition and in activation of the beta 2-adrenergic receptor. Proc. Natl. Acad. Sci. U.S.A. **93**, 9276–9281

12 Mitterdorfer, J., Froschmayr, M., Grabner, M., Striessnig, J. and Glossmann, H. (1994) Calcium channels: the β-subunit increases the affinity of dihydropyridine and Ca^{2+} binding sites of the α_1-subunit. FEBS Lett. **352**, 141–145

13 Striessnig, J. and Glossmann, H. (1991) Purification of L-type calcium channel drug receptors. Methods Neurosci. **4**, 210–229

14 Pichler, M., Cassidy, T. N., Reimer, D., Haase, H., Kraus, R., Ostler, D. and Striessnig, J. (1997) Beta subunit heterogeneity in neuronal L-type calcium channels. J. Biol. Chem. **272**, 13877–13882

15 DeLean, A., Munson, P. J. and Rodbard, D. (1978) Simultaneous analysis of families of sigmoid curves: application to bioassays, radioligand assay and physiological dose–response curves. Am. J. Physiol. **235**, E97–E102

16 Cheng, Y. and Prusoff, W. H. (1973) Relationship between the inhibition constant (K_i) and the concentration of inhibitor which causes 50 per cent inhibition (IC_{50}) of an enzymatic reaction. Biochem. Pharmacol. **22**, 3099–3108

17 Snutch, T. P., Tomlinson, W. J., Leonard, J. P. and Gilbert, M. M. (1991) Distinct calcium channels are generated by alternative splicing and are differentially expressed in the mammalian CNS. Neuron **7**, 45–57

18 Ito, H., Klugbauer, N. and Hofmann, F. (1997) Transfer of the high-affinity dihydropyridine sensitivity from L-type to non-L-type calcium channel. Mol. Pharmacol. **52**, 735–740

19 Hering, S., Aczel, S., Grabner, M., Döring, F., Berjukow, S., Mitterdorfer, J., Sinnegger, M. J., Striessnig, J., Degtiar, V. E., Wang, Z. and Glossmann, H. (1996) Transfer of high sensitivity for benzothiazepines from L-type to class A(BI) calcium channels. J. Biol. Chem. **271**, 24471–24475

20 King, V. F., Garcia, M. L., Himmel, D., Reuben, J. P., Lam, Y. T., Pan, J., Han, G. and Kaczorowski, G. J. (1988) Interaction of tetrandrine with slowly inactivating calcium channels. J. Biol. Chem. **263**, 2238–2244

21 Bezprozvanny, I. and Tsien, R. W. (1995) Voltage-dependent blockade of diverse types of voltage-gated Ca^{2+} channels expressed in *Xenopus* oocytes by the Ca^{2+} channel antagonist mibefradil (Ro 40–5967). Mol. Pharmacol. **48**, 540–549

22 Kraus, R. L., Hering, S., Grabner, M., Ostler, D. and Striessnig, J. (1998) Molecular mechanism of diltiazem interaction with L-type calcium channels. J. Biol. Chem. **273**, 27205–27212

23 Minor, D. L., Masseling, S. J., Jan, Y. N. and Jan, L. Y. (1999) Transmembrane structure of an inwardly rectifying potassium channel. Cell **96**, 879–891

24 Peterson, B. Z., Johnson, B. D., Hockerman, G. H., Acheson, M., Scheuer, T. and Catterall, W. A. (1997) Analysis of the dihydropyridine receptor site of L-type calcium channels by alanine-scanning mutagenesis. J. Biol. Chem. **272**, 18752–18758

25 Mitterdorfer, J., Wang, Z., Sinnegger, M. J., Hering, S., Striessnig, J., Grabner, M. and Glossmann, H. (1996) Two amino acid residues in the IIIS5 segment of L-type calcium channels differentially contribute to 1,4-dihydropyridine sensitivity. J. Biol. Chem. **271**, 30330–30335

26 Schuster, A., Lacinova, L., Klugbauer, N., Ito, H., Birnbaumer, L. and Hofmann, F. (1996) The IVS6 segment of the L-type calcium channel is critical for the action of dihydropyridines and phenylalkylamines. EMBO J. **15**, 2365–2370

27 Berger, W., Prinz, H., Striessnig, J., Kang, H.-C., Haugland, R. and Glossmann, H. (1994) A complex molecular mechanism for dihydropyridine binding to L-type calcium channels as revealed by fluorescence resonance energy transfer. Biochemistry **33**, 11875–11883

28 Brauns, T., Prinz, H., Kimball, S. D., Haugland, R. P., Striessnig, J. and Glossmann, H. (1997) L-type calcium channels: binding domains for dihydropyridines and benzothiazepines are located in close proximity to each other. Biochemistry **36**, 3625–3631

29 Striessnig, J., Goll, A., Moosburger, K. and Glossmann, H. (1986) Purified calcium channels have three allosterically coupled drug receptors. FEBS Lett. **197**, 204–210

30 Suh-Kim, H., Wei, X. and Birnbaumer, L. (1996) Subunit composition is a major determinant in high affinity binding of a calcium channel blocker. Mol. Pharmacol. **50**, 1330–1337

31 Chang, N., Lipkind, G., Fozzard, H., Penzotti, J., Sunami, A., French, R. and Dudley, S. (1999) Interactions with μ-Conotoxin GIIIA suggest a clockwise arrangement of the Na^+-channel domains. Biophys. J. **76**, 261 (abstract)

32 Welling, A., Ludwig, A., Zimmer, S., Klugbauer, N., Flockerzi, V. and Hofmann, F. (1997) Alternatively spliced IS6 segments of the alpha 1C gene determine the tissue-specific dihydropyridine sensitivity of cardiac and vascular smooth muscle L-type Ca^{2+} channels. Circ. Res. **81**, 526–532

33 Moebius, F. F., Burrows, G. G., Hanner, M., Schmid, E., Striessnig, J. and Glossmann, H. (1993) Identification of a 27 kDa-high affinity phenylalkylamine-binding polypeptide as the σ1 binding site, by photoaffinity labeling and ligand-directed antibodies. Mol. Pharmacol. **44**, 966–971

34 Moebius, F. F., Burrows, G. G., Striessnig, J. and Glossmann, H. (1993) Biochemical characterization of a 22-kDa high affinity antiischemic drug-binding polypeptide in the endoplasmic reticulum of guinea pig liver: potential common target for antiischemic drug action. Mol. Pharmacol. **43**, 139–148

35 Guy, H. R. and Conti, F. (1990) Pursuing the structure and function of voltage-gated channels. Trends Neurosci. **13**, 201–206

36 Schrempf, H., Schmidt, O., Kummerlen, R., Hinnah, S., Muller, D., Betzler, M., Steinkamp, T. and Wagner, R. (1995) A prokaryotic potassium ion channel with two predicted transmembrane segments from *Streptomyces lividans*. EMBO J. **14**, 5170–5178

37 Glossmann, H., Ferry, D. R., Luebbecke, F., Mewes, R. and Hofmann, F. (1982) Calcium channels: direct identification with radioligand binding studies. Trends Pharmacol. Sci. **3**, 431–437

38 Striessnig, J., Zernig, G. and Glossmann, H. (1985) Human red-blood-cell Ca^{2+}-antagonist binding sites. Eur. J. Biochem. **150**, 67–77

39 Boer, R., Grassegger, A., Schudt, C. and Glossmann, H. (1989) (+)-Niguldipine binds with very high affinity to Ca^{2+} channels and to a subtype of α1-adrenoceptors. Eur. J. Pharmacol. **172**, 131–145

Received 5 October 1999/3 February 2000; accepted 23 February 2000